# A mutant of the *Buthus martensii* Karsch antitumor-analgesic peptide exhibits reduced inhibition to hNa$_v$1.4 and hNa$_v$1.5 channels while retaining analgesic activity

Received for publication, April 21, 2017, and in revised form, September 6, 2017 Published, Papers in Press, September 18, 2017, DOI 10.1074/jbc.M117.792697

**Yijia Xu[‡], Xiangxue Meng[‡], Xue Hou[‡], Jianfang Sun[§], Xiaohua Kong[‡], Yuqi Sun[‡], Zeyu Liu[‡], Yuanyuan Ma[‡], Ye Niu[‡], Yongbo Song[‡], Yong Cui[¶], Mingyi Zhao[‡1], and Jinghai Zhang[¶2]**

*From the [‡]School of Life Sciences and Biopharmaceutical Science, Shenyang Pharmaceutical University, Shenyang, Liaoning 110016, the [§]College of Life and Health Sciences, Northeastern University, Shenyang, Liaoning 110004, and the [¶]School of Medical Devices, Shenyang Pharmaceutical University, Shenyang, Liaoning 110016, China*

Edited by F. Anne Stephenson

**Scorpion toxins can kill other animals by inducing paralysis and arrhythmia, which limits the potential applications of these agents in the clinical management of diseases. Antitumor-analgesic peptide (AGAP), purified from *Buthus martensii* Karsch, has been proved to possess analgesic and antitumor activities. Trp$^{38}$, a conserved aromatic residue of AGAP, might play an important role in mediating AGAP activities according to the sequence and homology-modeling analyses. Therefore, an AGAP mutant, W38G, was generated, and effects of both AGAP and the mutant W38G were examined by whole-cell patch clamp techniques on the sodium channels hNa$_v$1.4 and hNa$_v$1.5, which were closely associated with the biotoxicity of skeletal and cardiac muscles, respectively. The data showed that both W38G and AGAP inhibited the peak currents of hNa$_v$1.4 and hNa$_v$1.5; however, W38G induced a much weaker inhibition of both channels than AGAP. Accordingly, W38G exhibited much less toxic effect on both skeletal and cardiac muscles than AGAP *in vivo*. The analgesic activity of W38G and AGAP were verified *in vivo* as well, and W38G retained analgesic activity similar to AGAP. Inhibition to both Na$_v$1.7 and Na$_v$1.8 was involved in the analgesic mechanism of AGAP and W38G. These findings indicated that Trp$^{38}$ was a key amino acid involved in the biotoxicity of AGAP, and the AGAP mutant W38G might be a safer alternative for clinical application because it retains the analgesic efficacy with less toxicity to skeletal and cardiac muscles.**

Scorpion venom contains a large variety of biologically active components, including enzymes, peptides, nucleotides, lipids, mucoproteins, biogenic amines, and other unknown substances (1, 2), which might potentially act as new compounds in clinical medications, including epilepsy, convulsion, facial paralysis, hemiplegia, Parkinson's disease, tumor, and pain (3–11). In recent years, a range of scorpion analgesic peptides has been obtained and proved to target voltage-gated sodium channels (VGSCs),[3] such as *Buthus martensii* Karsch AngM1, *B. martensii* Karsch AGP-SYPU1, *B. martensii* Karsch AS, *B. martensii* Karsch BTx, and *Bm*NaL-3SS2 (12–15), although the exact interaction of toxins with VGSCs has remained unclear. Moreover, some severe adverse reactions have been caused, and the toxicological mechanism has been less explored despite the satisfactory analgesic effect of venoms (16).

VGSCs are considered to be involved in the generation and propagation action potential. Nine genes have been identified to encode functional sodium channel isoforms, namely Na$_v$1.1–Na$_v$1.9. Voltage-gated sodium channel 1.4 (Na$_v$1.4), encoded by *SCN4A*, is mainly expressed in skeletal muscle and essential for the generation and propagation of the action potential crucial to skeletal muscle contraction. Loss-of-function mutations in *SCN4A* lead to a decrease in peak sodium current ($I_{Nap}$), resulting in severe fetal hypokinesia or some classical congenital myopathy (17). The cardiac voltage-gated sodium channel (Na$_v$1.5) is encoded by *SCN5A* and mainly expressed in cardiac muscle. In the intercellular communication via gap junctions, Na$_v$1.5 is a major determinant of impulse conduction velocity in cardiac tissues (18). Loss-of-function mutations in *SCN5A* lead to defects in the generation and conduction of the cardiac electrical impulse and are associated with various arrhythmia phenotypes, including brugada syndrome, sick sinus syndrome, cardiac conduction diseases, and possibly dilated cardiomyopathy (19–22). Therefore, compounds blocking Na$_v$1.4 and Na$_v$1.5 might induce the dysfunction of muscular and cardiac system, leading to muscular and cardiac diseases and even death. Na$_v$1.4 and Na$_v$1.5 could also be viewed as one of the targets for the treatment of diseases associated with muscular and cardiac dysfunction. Some sodium channel isoforms have

This work was supported by National Key Scientific Project for New Drug Discovery and Development of China Grant 2014ZX09101044-001, National Natural Science Foundation of China Grant 81202855, Natural Science Foundation of Liaoning Province Grants 2015020726 and 2015020743, and Career Development Support Program of Shenyang Pharmaceutical University for Young and Middle-aged Teachers Grant 13. The authors declare that they have no conflicts of interest with the contents of this article.

This article contains supplemental Figs. S1–S3.

[1] To whom correspondence may be addressed: School of Life Sciences and Biopharmaceutical Science, Shenyang Pharmaceutical University, Shenyang, Liaoning 110016, China. Tel.: 86-024-23986431; Fax: 86-024-23986431; E-mail: zmy_dl@126.com.

[2] To whom correspondence may be addressed: School of Medical Devices, Shenyang Pharmaceutical University, Shenyang, Liaoning 110016, China. Tel.: 86-024-23986431; Fax: 86-024-23986431; E-mail: zhangjinghai@syphu.edu.cn.

[3] The abbreviations used are: VGSC, voltage-gated sodium channel; CK, creatine kinase; $I_{Nap}$, peak sodium current; LDH, lactate dehydrogenase; AGAP, antitumor-analgesic peptide; IMDM, Iscove's modified Dulbecco's medium; ANOVA, analysis of variance.

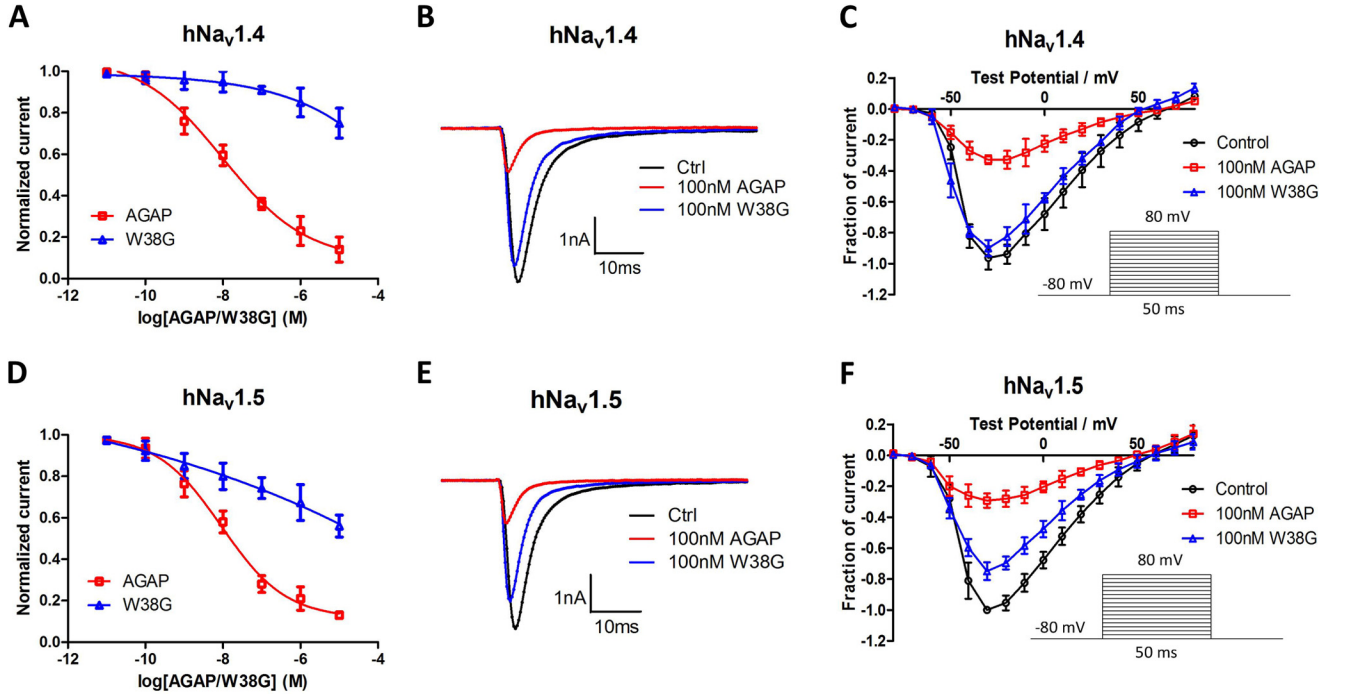


**Figure 1. Effects of AGAP and W38G on the $Na^+$ peak current of hNa$_v$1.4 and hNa$_v$1.5.** The $Na^+$ currents were obtained by plotting current peak amplitudes with a function of test potentials ranging from −80 to +80 mV for 50 ms from the holding potential of −80 mV in increments of 10 mV. Normalized $Na^+$ peak currents were depolarized at −20 mV after a 5-min treatment in the absence and presence of 10 pM, 100 pM, 1 nM, 10 nM, 100 nM, 1 μM, and 10 μM AGAP and W38G (*A* and *D*). The current traces were evoked by −20 mV for 50 ms from a holding potential of −80 mV in the absence and presence of 100 nM AGAP and W38G. Averaged current traces were obtained from hNa$_v$1.4-CHO (*B*) and hNa$_v$1.5-CHO (*E*) cells in each group. Current-voltage relationships of hNa$_v$1.4 (*C*) and hNa$_v$1.5 (*F*) were evoked by 100 nM AGAP and W38G. *, $p < 0.05$; **, $p < 0.01$; significant difference between AGAP and W38G values; paired one-way ANOVA. Each data point represents mean ± S.E. (*error bars*) ($n = 6$).

been reported to be potentially involved in the production of pain, of which Na$_v$1.7 and Na$_v$1.8 have drawn more attention because much evidence has been obtained of their close association with the triggering and propagation of pain.

Our group has been engaged in exploring new peptides from the Chinese scorpion *B. martensii* Karsch for many years. In previous studies (5, 23), antitumor-analgesic peptide (AGAP), one of the long-chain scorpion toxins purified from *B. martensii* Karsch, was proved to exhibit both analgesic and anti-tumor effects using *in vivo* models. Several site-directed mutations of AGAP were carried out based on the homology modeling and 3D structure analysis so as to improve its activity or decrease its toxicity (24) (supplemental Fig. S1). Among them, $Trp^{38}$, a conserved aromatic residue located in the core domain as well as a link between Face A and Face B, is assumed to be an important residue in maintaining AGAP function.

In this paper, the effects of an AGAP mutant, W38G, on both hNa$_v$1.4 and hNa$_v$1.5 were examined and compared with those of AGAP by using whole-cell patch clamp to evaluate its potential effects on the function of skeletal and cardiac muscles. The toxicity of W38G and AGAP on skeletal and cardiac muscles was examined *in vivo* as well, and the analgesic activity of W38G and AGAP was further verified by a thermal pain test and a formalin-induced paw-licking test. The results indicated that the mutant W38G displayed lower toxicities to skeletal and cardiac muscles than AGAP, whereas it retained an analgesic activity similar to that of AGAP. The decreased toxicity of W38G might result from its much lower inhibition of activities of both hNa$_v$1.4 (skeletal muscle) and hNa$_v$1.5 (cardiac muscle). Inhibition of the activities of both hNa$_v$1.7 and hNa$_v$1.8 might be involved in the analgesic mechanism of AGAP and W38G.

## Results

### *Effects of AGAP and W38G on hNa$_v$1.4 and hNa$_v$1.5*

*Effects of AGAP and W38G on the amplitude of sodium currents evoked from hNa$_v$1.4 and hNa$_v$1.5*—The effects of AGAP and W38G on the amplitude of sodium currents evoked from hNa$_v$1.4 and hNa$_v$1.5 expressed in CHO cells were determined and compared. Currents were elicited by test pulses ranging from −80 to +80 mV for 50 ms with increments of 10 mV. AGAP inhibited the amplitude of sodium currents in a concentration-dependent manner with a calculated $IC_{50}$ value of 10 nM for hNa$_v$1.4 and 12 nM for hNa$_v$1.5, respectively. The inhibition to hNa$_v$1.4 and hNa$_v$1.5 was significantly weakened by W38G with a calculated $IC_{50}$ value of 600 and 5 μM, respectively. Even at a concentration of 10 μM, the peak of the sodium currents was only inhibited by W38G to 75% for hNa$_v$1.4 and 56% for hNa$_v$1.5, respectively (Fig. 1, *A* and *D*).

At a concentration of 100 nM, AGAP potently inhibited the activity of both hNa$_v$1.4 and hNa$_v$1.5, with the amplitude of $I_{NaP}$ significantly reduced to 32 and 29%, respectively. As for W38G, the $I_{NaP}$ was only reduced to 90% on hNa$_v$1.4 and 75% on hNa$_v$1.5, which indicated a much weaker inhibition of both channels (Fig. 1) induced by W38G.

*Effects of AGAP and W38G on dynamic properties of hNa$_v$1.4 and hNa$_v$1.5*—The effects of AGAP and W38G were determined and compared on channel properties of hNa$_v$1.4 and

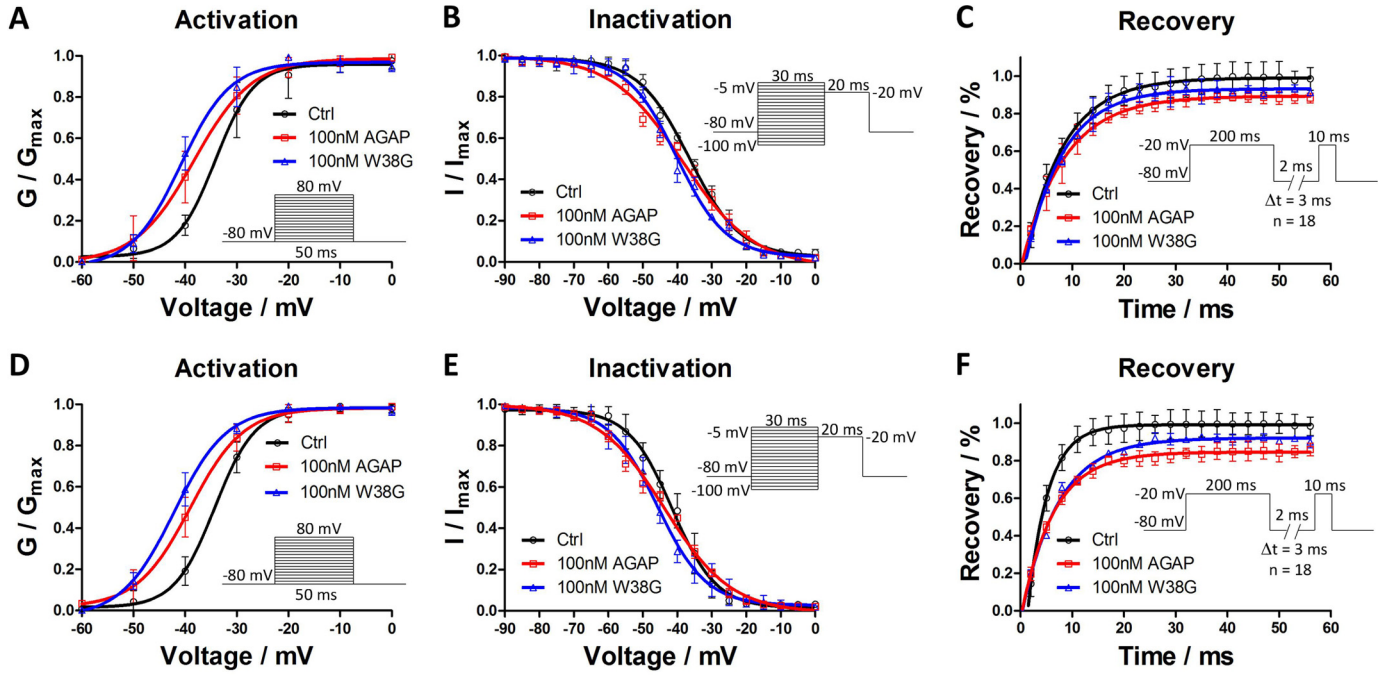


**Figure 2. Effects of AGAP and W38G on voltage dependence of activation and inactivation of hNa$_v$1.4 and hNa$_v$1.5 and effects of AGAP and W38G on recovery from inactivation of $Na^+$ current.** $Na^+$ current was generated by applying pulses from −80 to +40 mV at 10-mV steps for 20 ms from the holding potential of −80 mV in increments of 10 mV. Peak currents were converted into conductance, and normalized conductance of hNa$_v$1.4 (*A*) and hNa$_v$1.5 (*D*) was plotted against the voltages of conditioning pulses. Each point represents mean ± S.E. ($n = 6$). The currents were elicited with a test pulse at −20 mV for 20 ms following 30-ms prepulses ranging from −100 to 0 mV at 5-mV steps. Peak currents were normalized, and the inactivation curves of hNa$_v$1.4 (*B*) and hNa$_v$1.5 (*E*) were plotted against the command potentials. Each point represents mean ± S.E. (*error bars*) ($n = 6$). The currents were obtained at two pulses, consisting of a 200-ms prepulse to −20 mV followed by resting at −80 mV for a time varying from 2 to 56 ms in increments of 3 ms and a test pulse to −20 mV for 10 ms. The $I/I_{max}$ ratio represented the recovery of $Na^+$ current from inactivation for hNa$_v$1.4 (*C*) and hNa$_v$1.5 (*F*). Each point represents mean ± S.E. ($n = 6$).

hNa$_v$1.5. After exposure to 100 nM AGAP, the *I*-V curve was significantly shifted to the hyperpolarized direction with $V_{½}$ values of activation decreased by 4.1 mV on hNa$_v$1.4 and 5.1 mV on hNa$_v$1.5. The slope factor was also changed by 1.9 and 1.5 against the control, respectively. 100 nM W38G shifted the $V_{½}$ of activation by −6.6 mV on hNa$_v$1.4 and −8.4 mV on hNa$_v$1.5 with few changes of the slope factors compared with the control (Fig. 2 (*A* and *D*) and Table 1). With regard to the inactivation phase, a 100 nM concentration of either AGAP or W38G had no significant effect on $V_{½}$ values of inactivation on both hNa$_v$1.4 and hNa$_v$1.5. AGAP evoked a change of slope factor by 3.4 for hNa$_v$1.5 compared with control, whereas W38G evoked few changes of the slope factor for both hNa$_v$1.4 and hNa$_v$1.5. Both hNa$_v$1.4 and hNa$_v$1.5 were somewhat difficult to recover from inactivation to resting state after exposure to 100 nM AGAP and W38G, although the duration of the recovery process changed little (Fig. 2, *C* and *F*).

Compared with AGAP, W38G exhibited a similar effect on $V_{½}$ values of hNa$_v$1.4 and hNa$_v$1.5 in both activation and inactivation phases with no significant differences. W38G exhibited the same effect in the recovery phase from the inactivated state to the resting state. The activation, inactivation, and recovery parameters are summarized in Table 1.

### *Toxicity of AGAP and W38G to skeletal and cardiac muscle in vivo*

*Acute toxicity of AGAP and W38G to skeletal and cardiac muscle in vivo*—Due to the much less inhibitory effects on hNa$_v$1.4 and hNa$_v$1.5 *in vitro*, W38G is assumed to be a potential toxin analog with lower side effects on the cardiac and muscular system. In a previous study, AGAP showed distinct analgesic activity at a concentration of 0.5 mg/kg. Therefore, doses up to 5- and 10-fold higher were used to examine the potential muscular and cardiac toxicity of AGAP and W38G in mice. As shown in Fig. 3, 2.5 mg/kg AGAP and 2.5 and 5.0 mg/kg W38G exhibited no significant effects on heart rate compared with saline control. By contrast, 5.0 mg/kg AGAP decreased the heart rate at 15 min after intravenous injection. 2.5 and 5.0 mg/kg W38G had no effects on activity levels of creatine kinase (CK) and lactate dehydrogenase (LDH) as well, whereas both 2.5 and 5.0 mg/kg of AGAP significantly increased the activity levels of CK and LDH, indicating that potential damage to skeletal or cardiac muscle was induced by AGAP.

*Subacute toxicity of AGAP and W38G to skeletal and cardiac muscle in vivo*—Survival analysis was carried out, and survival curves of 20 mice in each group are shown in Fig. 4. At doses of 2.5 mg/kg, all mice died by the day 6 in the AGAP-treated group, whereas 16 mice survived in the W38G-treated group (Fig. 4*A*). At doses of 5.0 mg/kg, all mice died by day 4 in the AGAP-treated group, whereas four mice survived in the W38G-treated group (Fig. 4*B*). A log-rank test of the survival analysis showed a rather lower toxicity of W38G than of AGAP, although 5.0 mg/kg W38G still retained considerable toxicity when continuously administered to mice.

Mice surviving a 7-day treatment of 2.5 mg/kg W38G or the same amount of saline were randomly and equally divided into two groups, respectively. To investigate the effect of W38G on

**Table 1**

**Effects of AGAP and W38G on the kinetic and recovery properties of hNa$_v$1.4 and hNa$_v$1.5**

*, $p < 0.05$; significant difference between control and toxins on hNa$_v$1.4 and hNa$_v$1.5; one-way ANOVA. #, $p < 0.05$; significant difference between AGAP and W38G on hNa$_v$1.4 and hNa$_v$1.5; one-way ANOVA. **, $p < 0.01$; significant difference between control and toxins on hNa$_v$1.4 and hNa$_v$1.5; one-way ANOVA. ##, $p < 0.01$; significant difference between AGAP and W38G on hNa$_v$1.4 and hNa$_v$1.5; one-way ANOVA.

| | hNa$_v$1.4 | | | hNa$_v$1.5 | | |
|---|---|---|---|---|---|---|
| Group | Control | AGAP (100 nM) | W38G (100 nM) | Control | AGAP (100 nM) | W38G (100 nM) |
| **Activation** | | | | | | |
| $V_{½}$ (mV) | −34.18 ± 0.65 | −38.31 ± 0.36* | −40.81 ± 0.76* | −34.29 ± 0.26 | −39.35 ± 0.26* | −42.66 ± 0.31*# |
| $k$ | 3.75 ± 0.24 | 5.66 ± 0.73* | 4.81 ± 0.24* | 3.90 ± 0.28 | 5.42 ± 0.25* | 4.47 ± 0.26 |
| **Inactivation** | | | | | | |
| $V_{½}$ (mV) | −36.48 ± 0.67 | −37.31 ± 0.32 | −39.40 ± 0.72 | −42.09 ± 0.34 | −43.67 ± 0.71 | −45.73 ± 0.69 |
| $k$ | 8.78 ± 0.62 | 8.90 ± 0.33 | 7.64 ± 0.36 | 6.25 ± 0.28 | 9.68 ± 0.69* | 7.06 ± 0.55 |
| **Recovery** | | | | | | |
| $\tau$(ms) | 7.51 ± 0.53 | 8.21 ± 0.46 | 7.56 ± 0.51 | 4.32 ± 0.66 | 6.26 ± 0.45 | 7.09 ± 0.49* |

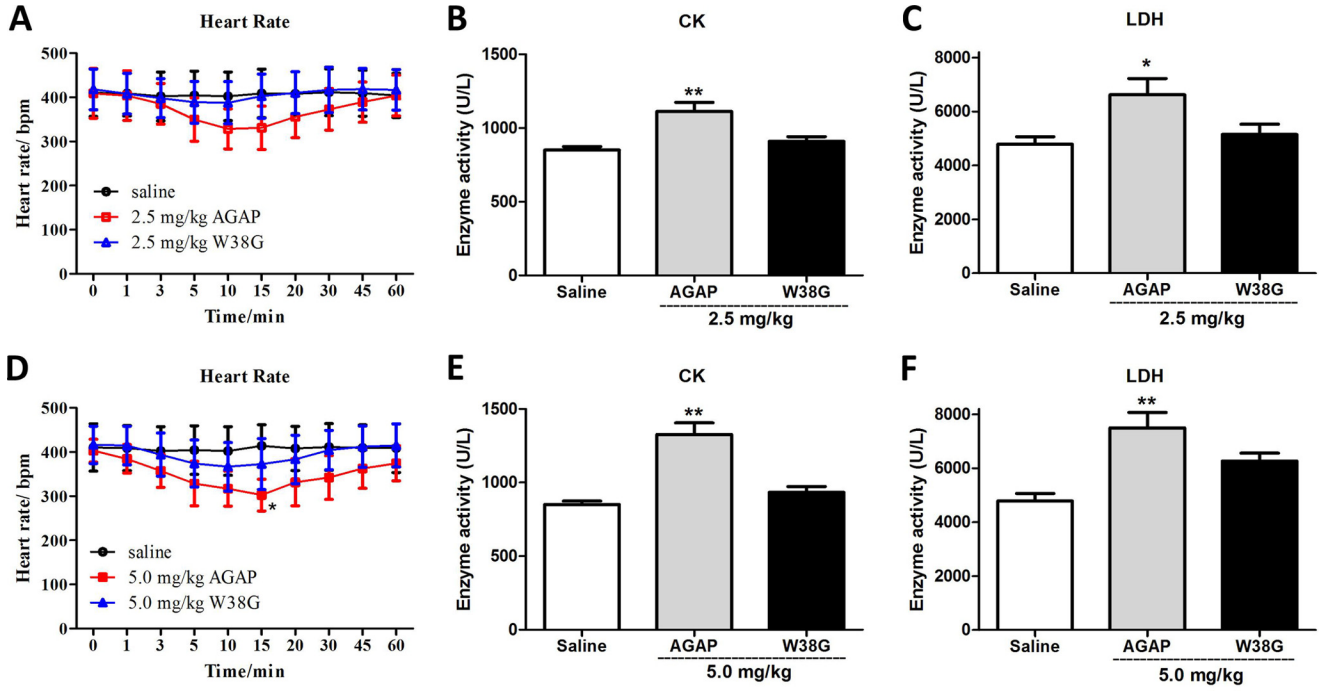


**Figure 3. The effects of AGAP and W38G on heart rate (*A* and *D*) and enzyme activities (*B*, *C*, *E*, and *F*) of CK and LDH at doses up to 2.5 and 5.0 mg/kg.** In each experiment, data points represent mean ± S.E. (*error bars*) ($n = 10$ for saline and 2.5 mg/kg W38G, $n = 8$ for 5.0 mg/kg W38G, $n = 6$ for 2.5 mg/kg AGAP, $n = 4$ for 5.0 mg/kg AGAP). Statistically significant differences compared with the saline control group (calculated using one-way ANOVA) are indicated by $p < 0.05$ (*) or $p < 0.01$ (**).

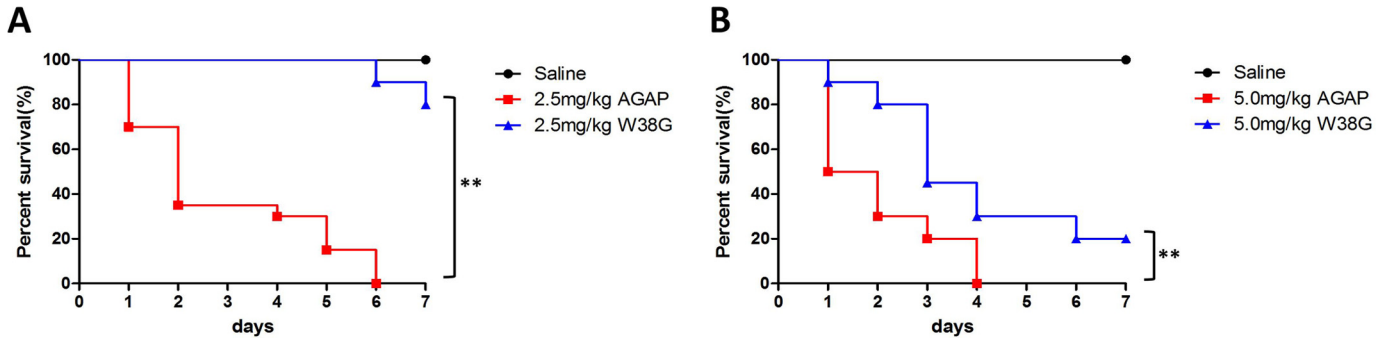


**Figure 4. One-week survival of mice treated with AGAP and W38G.** W38G improves survival time of AGAP at doses of 2.5 and 5.0 mg/kg with 20 mice in each group. Mice treated with normal saline are shown as a comparison. Comparison of the survival curves of the AGAP and W38G groups was calculated using log-rank test analysis. *, $p < 0.05$; **, $p < 0.01$; statistically significant differences.

motor functions in mice, the forced swimming test and rotarod test were administered immediately 20 min after the last injection on day 7. A corresponding amount of saline was injected in the exact same way as the control. The data showed that the accumulation of W38G did not affect the motor functions of mice in both the forced swimming test and rotarod test compared with control (Fig. 5, *A* and *B*). No significant differences were found between the W38G-treated group and the control

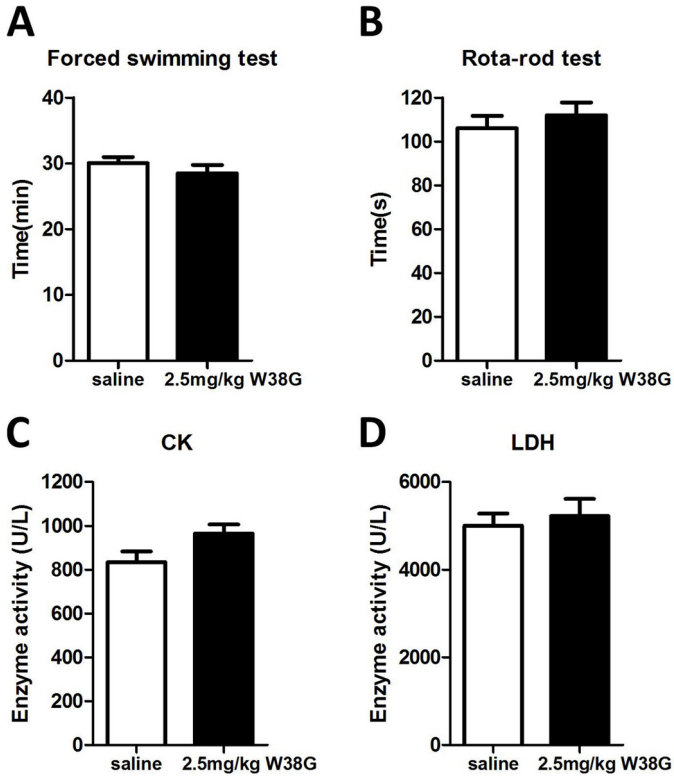


**Figure 5. The effects of W38G on motor function (*A* and *B*) and enzyme activities (*C* and *D*) of CK and LDH after intravenous injection for 7 days.** In each experiment, data points represent mean ± S.E. (*error bars*) ($n = 10$ for saline, $n = 8$ for 2.5 mg/kg W38G). Statistically significant differences compared with the saline control group (calculated using one-way ANOVA) are indicated by $p < 0.05$ (*) and $p < 0.01$ (**).

group with reference to the activity levels of serum CK and LDH (Fig. 5, *C* and *D*). These results indicated that 2.5 mg/kg W38G caused much lower toxicities to skeletal and cardiac muscles even after 7-day treatment.

### *Analgesic activities of W38G compared with AGAP in vivo*

Analgesic effects of AGAP and W38G were further verified in rodent pain models induced by heat or noxious chemical.

W38G similarly reduced the pain induced by a hot plate when compared with AGAP. The licking time increased significantly in a concentration-dependent method in both AGAP-treated groups and W38G-treated groups. By 15 min, the licking time of mice had increased from 9.5 to 17.6 s (0.25 mg/kg), 24.5 (0.5 mg/kg), and 28.3 s (1.0 mg/kg) in the AGAP-treated group, whereas those times had increased from 10.6 to 19.7 s (0.25 mg/kg), 28.7 s (0.5 mg/kg), and 31.5 s (1.0 mg/kg) in the W38G-treated group. By 45 min, the licking time of mice had increased from 9.5 to 17.3 s (0.25 mg/kg), 26.7 s (0.5 mg/kg), and 27.4 s (1.0 mg/kg) in the AGAP-treated group, whereas those times had increased from 10.6 to 19.3 s (0.25 mg/kg), 29.2 s (0.5 mg/kg), and 31.2 s (1.0 mg/kg) in the W38G-treated group (Fig. 6*A*). The analgesic effect of AGAP and W38G initiated at 15 min and was sustained until 60 min or longer in the hot-plate model (Fig. 6*B*).

Intraplantar injection of formalin can produce two phases of nociceptive behaviors in mice. The nociceptive behaviors in the first phase (0–5 min postinjection), was caused by direct stimulation of TRPA1 in a subpopulation of C-fiber nociceptors and followed by a quiescent period. The nociceptive behaviors in the second phase (20–40 min postinjection) were caused by peripheral inflammation together with central nervous sensitization. Nociceptive responses were relieved significantly and dose-dependently in both phase I and phase II by intravenous injection of AGAP and W38G (Fig. 6, *C* and *D*). In phase I, the average licking time was significantly attenuated to 76.2, 63.9, and 54.8% of that in control group by 0.25, 0.5, and 1.0 mg/kg AGAP and 69.7, 58.7, and 53.7% of that in control group by 0.25, 0.5, and 1.0 mg/kg W38G (Fig. 6*C*). This time was also attenuated for AGAP and W38G in phase II, with a rate of 95.1, 73.6, and 60.5% and 92.9, 69.6, and 54.7% at concentrations of 0.25, 0.5, and 1.0 mg/kg, respectively (Fig. 6*D*).

### *Effects of AGAP and W38G on hNa$_v$1.7 and hNa$_v$1.8*

To explore the possible mechanisms for analgesic activities, effects of AGAP and W38G were examined on the activity of hNa$_v$1.7 and hNa$_v$1.8. At a concentration of 100 nM, AGAP potently inhibited the activity of both hNa$_v$1.7 and hNa$_v$1.8, with the amplitude of $I_{NaP}$ significantly reduced to 32 and 75%, respectively. As for W38G, the amplitude of $I_{NaP}$ was reduced to 57% on hNa$_v$1.7 and 80% on hNa$_v$1.8. It seemed that W38G induced a weaker inhibition to hNa$_v$1.7 than AGAP (Fig. 7), whereas it induced a similar inhibition to hNa$_v$1.8 with AGAP (Fig. 8).

After exposure to 100 nM AGAP, the *I*-V curve was significantly shifted to the hyperpolarized direction with $V_{½}$ values of activation decreased by 6.0 mV on hNa$_v$1.7 and 3.9 mV on hNa$_v$1.8. Few changes of the slope factors were evoked by AGAP on both hNa$_v$1.7 and hNa$_v$1.8. 100 nM W38G shifted the $V_{½}$ values of activation by −8.0 mV on hNa$_v$1.7 and −5.7 mV on hNa$_v$1.8 with few changes of the slope factors compared with the control (Figs. 7*C* and 8*C*) (Table 2). With regard to the inactivation phase, a 100 nM concentration of either AGAP or W38G had no significant effect on $V_{½}$ values and slope factors on both hNa$_v$1.7 and hNa$_v$1.8 (Figs. 7*D* and 8*D*) (Table 2).

## Discussion

Scorpion toxins can prolong the action potentials of excitable cells *in vivo* and kill other animals by inducing paralysis and arrhythmia, which contributes greatly to their major toxicity. According to the size of the peptide chain, scorpion toxins can be characterized as short-chain toxins, usually targeting potassium channels, and long-chain toxins, usually targeting sodium channels (25, 26). *B. martensii* Karsch AGAP is composed of 66 amino acids and viewed as a long-chain toxin, although the association of its function with sodium channels has not yet been elucidated clearly.

In this study, Na$_v$1.4 and Na$_v$1.5 were considered as the targets to screen the possible toxicity to skeletal and cardiac muscles due to their specific distributions and roles in maintaining the skeletal and cardiac electrophysiology. Effects of AGAP and its several mutants were first examined on the amplitude of sodium channel currents evoked from hNa$_v$1.4 and hNa$_v$1.5 expressed in CHO cells. W38G was selected to be further studied due to its distinctly reduced inhibition to both hNa$_v$1.4 and hNa$_v$1.5 at a concentration of 100 nM (supplemental Fig. S2).

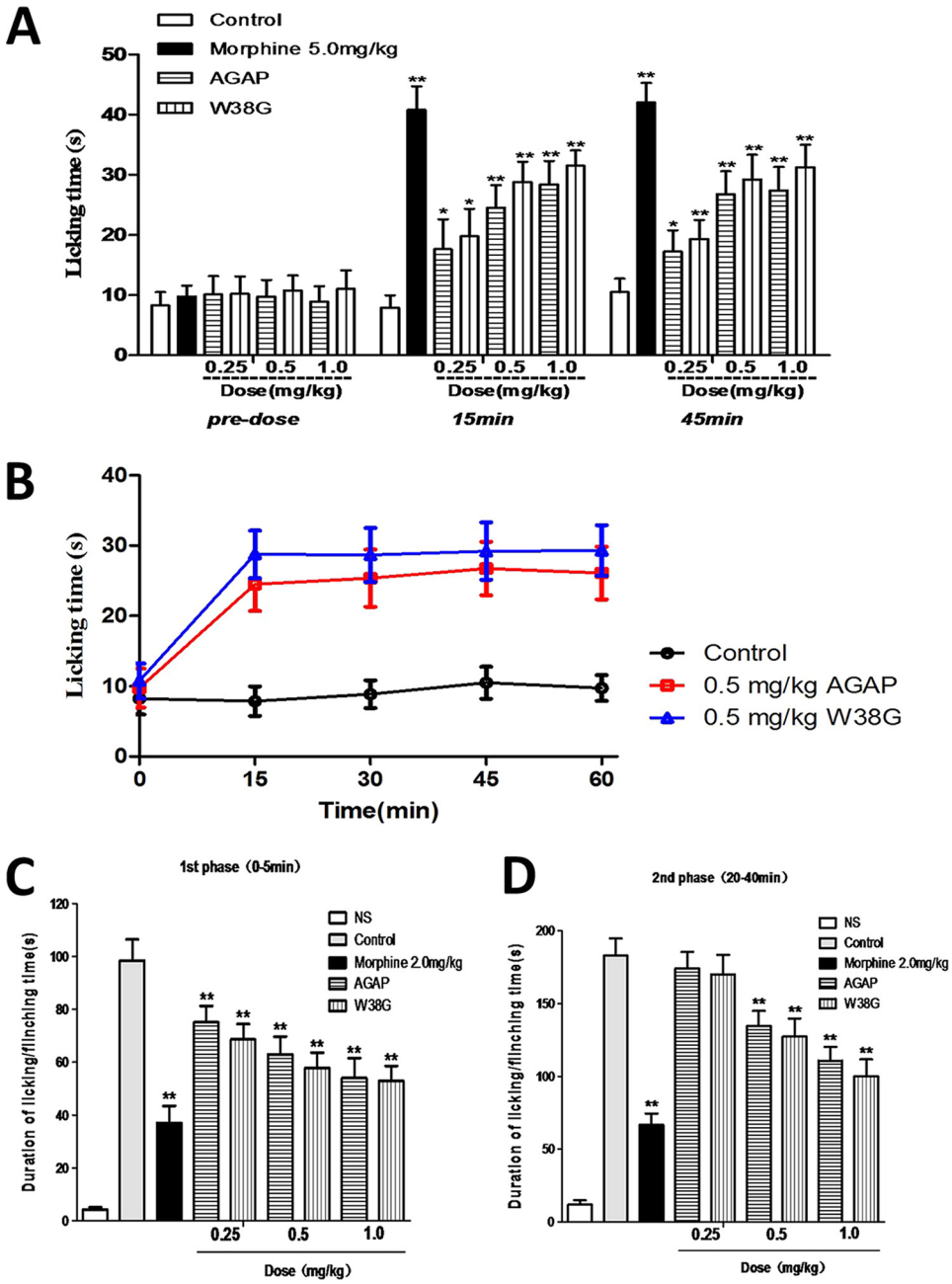


**Figure 6. Analgesic effects of AGAP and W38G in mice.** Both AGAP and W38G have analgesic effects in rodent pain models. W38G was similarly effective as AGAP at reducing thermal-induced pain (*A* and *B*). W38G was similarly effective as AGAP in attenuating nociceptive behavior (duration of paw licking and flinching time) during phase I (0–5 min postinjection) (*C*) and phase II (20–40 min postinjection) (*D*) following intraplantar injection of formalin. Data points are shown as mean ± S.E. (*error bars*) ($n = 10$). Statistically significant differences compared with the saline control group (calculated using one-way ANOVA) are indicated by $p < 0.05$ (*) and $p < 0.01$ (**).

The data in this study showed that AGAP displayed a significantly inhibitory effect on both hNa$_v$1.4 and hNa$_v$1.5, which might contribute to its toxicity to skeletal and cardiac muscles. The W38G mutation significantly decreased the inhibition of $I_{Nap}$ with the calculated $IC_{50}$ value increased 60,000-fold for hNa$_v$1.4 and 420-fold for hNa$_v$1.5 (Fig. 1). However, the kinetic characteristics of both channels evoked by W38G exhibited a variation similar to that evoked by AGAP, including activation, inactivation, and recovery process. Therefore, the reduced inhibition of W38G to hNa$_v$1.4 and hNa$_v$1.5 seemed more likely to be due to its decreased blocking action on both channels than its changes on kinetic processes. These results indicated that $Trp^{38}$ might be the key amino acid to maintain the crucial structure of AGAP interacting with hNa$_v$1.4 and hNa$_v$1.5. Also, the structural nuances of AGAP and W38G might explain their different performance on channels, because W38G had been proved to change the CD spectra of AGAP in a previous study (24). A detailed comparison of the surface formed by the interaction of toxins with VGSCs might be necessary to validate this hypothesis; however, this seemed difficult to carry out in the current work.

Due to its weakened inhibition to Na$_v$1.4 and Na$_v$1.5, W38G is assumed to possess lower adverse effects on the muscular and cardiac system. Acute and subacute experiments were carried

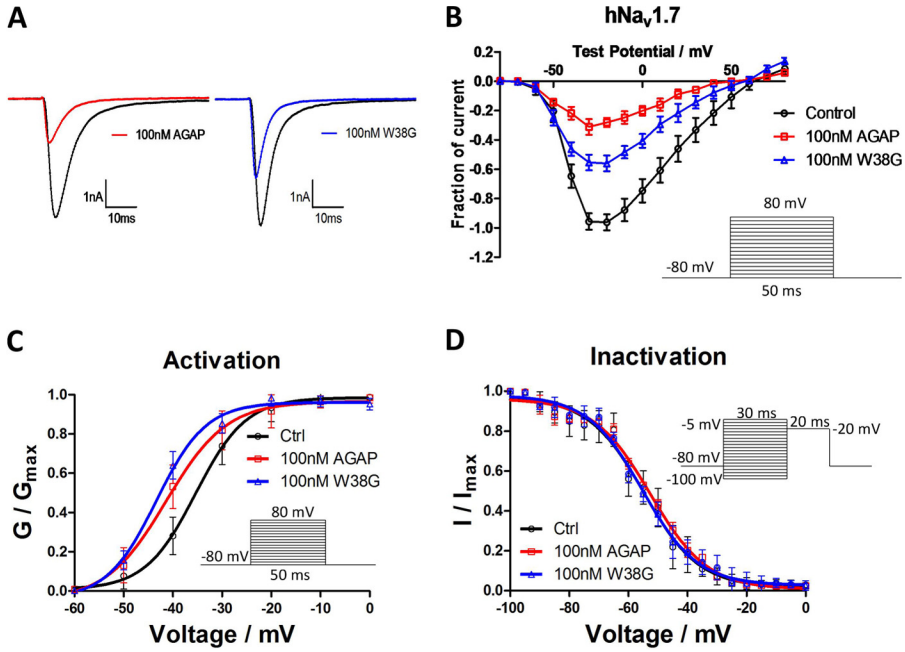


**Figure 7. Effects of AGAP and W38G on hNa$_v$1.7.** The $Na^+$ currents were obtained by plotting current peak amplitudes with a function of test potentials ranging from −80 to +80 mV for 50 ms from the holding potential of −80 mV in increments of 10 mV. The current traces were evoked by −20 mV for 50 ms from a holding potential of −80 mV in the absence and presence of 100 nM AGAP and W38G. Averaged current traces were obtained from hNa$_v$1.7 (*A*) cells in each group. The current-voltage relationship of hNa$_v$1.7 (*B*) was evoked by 100 nM AGAP and W38G. Peak currents were converted into conductance, and normalized conductance of hNa$_v$1.7 (*C*) was plotted against the voltages of conditioning pulses. The currents were elicited with a test pulse at −20 mV for 20 ms following 30-ms prepulses ranging from −100 to 0 mV at 5-mV steps. Peak currents were normalized, and the inactivation curves of hNa$_v$1.7 (*D*) were plotted against the command potentials. Each data point represents mean ± S.E. (*error bars*) ($n = 6$).

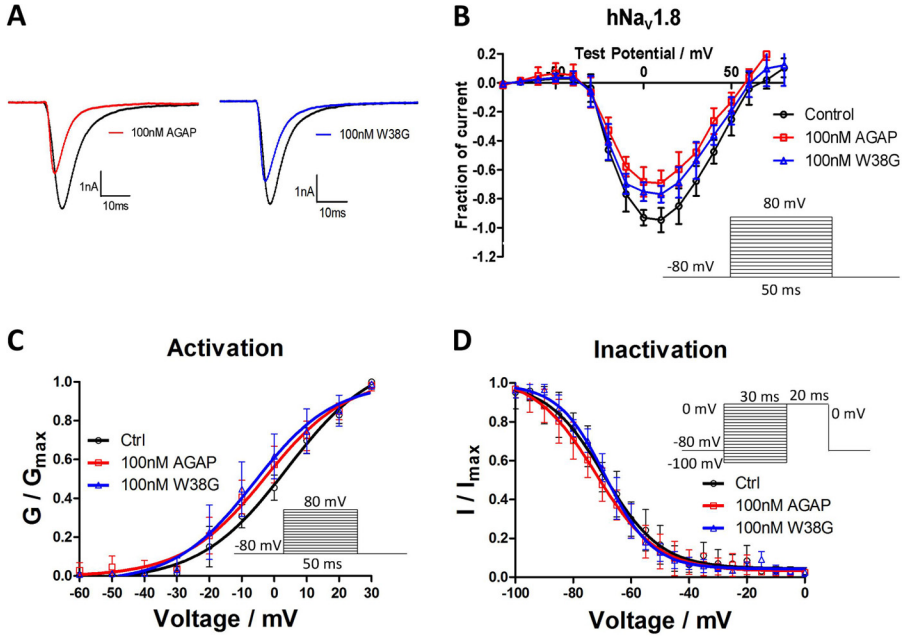


**Figure 8. Effects of AGAP and W38G on hNa$_v$1.8.** The $Na^+$ currents were obtained by plotting current peak amplitudes with a function of test potentials ranging from −80 to +80 mV for 50 ms from the holding potential of −80 mV in increments of 10 mV. The current traces were evoked by +10 mV for 50 ms from a holding potential of −80 mV in the absence and presence of 100 nM AGAP and W38G. Averaged current traces were obtained from hNa$_v$1.8 (*A*) cells in each group. The current-voltage relationship of hNa$_v$1.8 (*B*) was evoked by 100 nM AGAP and W38G. Peak currents were converted into conductance, and normalized conductance of hNa$_v$1.8 (*C*) was plotted against the voltages of conditioning pulses. The currents were elicited with a test pulse at +10 mV for 20 ms following 30-ms prepulses ranging from −100 to 0 mV at 5-mV steps. Peak currents were normalized, and the inactivation curves of hNa$_v$1.8 (*D*) were plotted against the command potentials. Each data point represents mean ± S.E. (*error bars*) ($n = 5$).

out to verify this assumption. Heart rate is the most direct measure for arrhythmia. CK and LDH exist in higher amounts in the cytoplasm and mitochondria of cardiac and skeletal muscle cells. Increased activity levels of CK and LDH in serum are commonly considered as a highly specific and sensitive measure of muscle cell death (27, 28), such as in the presence of acute myocardial infarction and skeletal muscle damage (29–32). In this study, W38G exhibited no significant effects on

**Table 2**
**Effects of AGAP and W38G on the kinetic of hNa$_v$1.7 and hNa$_v$1.8**

*, $p < 0.05$; significant difference between control and toxins on hNa$_v$1.7 and hNa$_v$1.8; one-way ANOVA. #, $p < 0.05$; significant difference between AGAP and W38G on hNa$_v$1.7 and hNa$_v$1.8; one-way ANOVA. **, $p < 0.01$; significant difference between control and toxins on hNa$_v$1.7 and hNa$_v$1.8; one-way ANOVA. ##, $p < 0.01$; significant difference between AGAP and W38G on hNa$_v$1.7 and hNa$_v$1.8; one-way ANOVA.

| | hNa$_v$1.7 | | | hNa$_v$1.8 | | |
|---|---|---|---|---|---|---|
| Group | Control | AGAP (100 nM) | W38G (100 nM) | Control | AGAP (100 nM) | W38G (100 nM) |
| **Activation** | | | | | | |
| $V_{½}$ (mV) | −35.38 ± 0.33 | −41.35 ± 0.78* | −43.35 ± 0.95* | 0.79 ± 0.55 | −3.13 ± 0.75* | −4.88 ± 0.9* |
| $k$ | 5.11 ± 0.27 | 6.15 ± 0.69 | 5.05 ± 0.78 | 10.77 ± 0.5 | 11.39 ± 0.68 | 11.35 ± 0.8 |
| **Inactivation** | | | | | | |
| $V_{½}$ (mV) | −54.81 ± 0.98 | −52.60 ± 0.82 | −55.24 ± 0.70 | −67.84 ± 0.63 | −70.16 ± 0.56 | −67.8 ± 0.48 |
| $k$ | 9.34 ± 0.92 | 9.65 ± 0.77 | 9.33 ± 0.65 | 10.93 ± 0.57 | 10.84 ± 0.52 | 9.15 ± 0.44 |

heart rate, activity levels of CK and LDH, and motor function in both acute and subacute toxicity tests, whereas 5.0 mg/kg AGAP decreased the heart rate at 15 min after intravenous injection and significantly increased the activity levels of CK and LDH in the serum of mice. In survival analysis, mice in W38G-treated groups survived much longer than those in AGAP-treated groups. Although the half-life of most peptides is generally short, the toxicity induced by AGAP indicated an accumulation of AGAP by continuous administration. The results confirmed that W38G exhibited much lower toxicity to skeletal and cardiac muscles compared with AGAP. Although multiple complicated mechanisms might be involved in the reduced toxicity of W38G *in vivo*, the decreased inhibition of hNa$_v$1.4 and hNa$_v$1.5 was assumed to be one major reason.

In this study, W38G and AGAP exhibited similar analgesic effects in rodent pain models induced by heat and noxious chemicals; however, the analgesic mechanism remains uncertain. Na$_v$1.7 and Na$_v$1.8 are the most prominent potential targets associated closely with both acute and chronic pain. Na$_v$1.7, one of the tetrodotoxin-sensitive voltage-gated sodium channel isoforms, is abundantly expressed in dorsal root ganglion and sympathetic ganglion pain-sensing neurons (33–35). In recent years, Na$_v$1.7 has been thought to be a major contributor to pain signaling in humans, according to genetic and functional studies (36–39), and to be associated with erythromelalgia, paroxysmal extreme pain disorder, and congenital insensitivity to pain (39, 40). Na$_v$1.8, one of the tetrodotoxin-resistant voltage-gated sodium channel isoforms, is prominently expressed in primary sensory neurons, including dorsal root ganglion neurons (41, 42). A previous study (43) showed that knockdown of Na$_v$1.8 can attenuate neuropathic and inflammatory pain in rodents. AGAP potently inhibited the activity of both hNa$_v$1.7 (Fig. 7) and hNa$_v$1.8 (Fig. 8), indicating that both channel isoforms were involved in the analgesic mechanism of AGAP. W38G evoked a similar inhibitory effect on hNa$_v$1.8 but a much weaker inhibition of hNa$_v$1.7 compared with AGAP. Considering the similar analgesic effects, it seemed that the inhibition of hNa$_v$1.8 might be more responsible for the analgesic effects of AGAP exhibited in rodent pain models induced by heat and noxious chemicals.

Another notable point is that AGAP had been defined as an $\alpha$-type scorpion toxin by the bioinformational analysis of the structure in a previous study (5). However, one of the characteristics of $\alpha$-type scorpion toxins is that they are well-known to affect the inactivation process of VGSCs in excitable membranes by binding to receptor site 3. In this study, AGAP induced little changes in the inactivation processes of hNa$_v$1.4, hNa$_v$1.5, hNa$_v$1.7, and hNa$_v$1.8. On the contrary, the activation processes of these four channels were changed with *I*-V curves left-shifted to the hyperpolarized direction after exposure to 100 nM AGAP (Figs. 2, 7, and 8). A prepulse protocol was used to determine whether AGAP is a $\beta$-type scorpion toxin (44). The current-voltage relationships for AGAP-modified sodium currents were analyzed and revealed a negative shift in the voltage dependence of activation after priming depolarizations in the presence of AGAP (supplemental Fig. S3). Therefore, it is more reasonable to define AGAP as a $\beta$-type scorpion toxin rather than an $\alpha$-type toxin according to its electrophysiological characteristics upon the interaction with hNa$_v$1.4, hNa$_v$1.5, hNa$_v$1.7, and hNa$_v$1.8. More evidence should be obtained in further studies to verify this assumption.

In conclusion, the mutant W38G exhibited much lower inhibitory effects on hNa$_v$1.4 and hNa$_v$1.5 compared with AGAP. Correspondingly, W38G displayed much lower toxicities to skeletal and cardiac muscles than AGAP, whereas it retained analgesic activity similar to that of AGAP *in vivo*. Na$_v$1.7 and Na$_v$1.8 might be involved in the analgesic mechanism of AGAP and W38G, indicating that the conserved Trp$^{38}$ might be a key amino acid involved in the biotoxicity and bioactivity of AGAP, and mutant W38G might be a safer alternative for clinical use because it retains pharmaceutical efficacy with few adverse effects. These findings might facilitate the modification of other scorpion toxins with high preference for their bioactivity target with lower side effects as well.

## Experimental procedures

### *Animals*

Healthy female and male Kunming mice were obtained from the Experimental Animal Center of Shenyang Pharmaceutical University (Shenyang, China). They were maintained in standard laboratory conditions of temperature 25 ± 1 °C and a 12-h light/12-h dark cycle with free access to food and water for the duration of the study. The mice were acclimatized for 2 weeks before all tests. Animal care was in accordance with the Guidelines for Animal Experimentation of Shenyang Pharmaceutical University, and the protocol was approved by the Animal Ethics Committee of the institution. All of the cells and tissues of the mice were authorized to be used for scientific purposes.

### *Cell cultures*

IMDM, DMEM, 0.25% trypsin-EDTA, FBS, penicillin/streptomycin, HT supplement, GlutaMAX, and hygromycin were

obtained from Life Technologies, Inc., and G418 was purchased from Calbiochem. CHO cells were cultured in IMDM with 2 mM GlutaMAX and supplemented with 100 $\mu$M hypoxanthine, 16 $\mu$M thymidine, and 10% FBS. ND7/23 cells were cultured in DMDM with 2 mM GlutaMAX and 10% FBS. hNa$_v$1.4-CHO, hNa$_v$1.5-CHO, and hNa$_v$1.7-CHO cells were cultured in IMDM with 2 mM GlutaMAX and supplemented with 100 $\mu$M hypoxanthine, 16 $\mu$M thymidine, 10% FBS, and 200 $\mu$g/ml G418. hNa$_v$1.8-ND7/23 cells were cultured in DMDM with 2 mM GlutaMAX, 10% FBS, and 200 $\mu$g/ml hygromycin. All cells were cultured routinely as monolayers on a poly-D-lysine–coated dish in an atmosphere of 5% $CO_2$ and 37 °C.

### *Purification of recombinant scorpion toxins*

*Escherichia coli* BL21 (DE3) cells harboring expression vectors of pSYPU/AGAP(W38G) were grown and harvested as described previously (5), following purification by nickel metal chelating ion affinity chromatography. All purified toxins were analyzed by SDS-PAGE and diluted in external solution/normal saline for the whole-cell patch clamp/animal tests.

### *Automated patch clamp electrophysiology recording*

Whole-cell patch clamp recording was used to examine functional properties of hNa$_v$1.4-CHO, hNa$_v$1.5-CHO, hNa$_v$1.7-CHO, and hNa$_v$1.8-ND7/23 cell lines using an automated electrophysiology platform (NPC-1 and Port-a-patch system, Nanion Technologies GmbH, Munich, Germany) and an EPC10 Amplifier (HEKA Elektronik, Lambrecht, Germany). Cells were detached with 0.25% trypsin-EDTA, terminated in fresh culture medium, centrifuged (100 × *g*, 3 min), and resuspended in external solution to reach a density of $1 \times 10^6$ cells/ml. Patchcontrol HT software (Nanion Technologies) was used to control the application of solutions and pressures necessary to establish the whole-cell configuration. Sodium currents were recorded at room temperature (20–25 °C) using external (140 mM NaCl, 4 mM KCl, 1 mM $MgCl_2$, 2 mM $CaCl_2$, 5 mM D-glucose monohydrate, 10 mM HEPES/NaOH, pH 7.4) and internal solutions (50 mM CsCl, 10 mM NaCl, 60 mM CsF, 20 mM EGTA, 10 mM HEPES/CsOH, pH 7.2) identical to those used for conventional patch clamp experiments. Following cell contact with the 2–3.5–megaohm planar electrode, seal enhancer solution (80 mM NaCl, 3 mM KCl, 35 mM $CaCl_2$, 10 mM $MgCl_2$, 10 mM HEPES/NaOH, pH 7.4) was added to the external solution to promote gigaohm seal formation. After establishing the whole-cell configuration, the seal enhancer solution was replaced with two washes of fresh external solution, and the series resistance was compensated automatically. Patchmaster software (HEKA Elektronik, Lambrecht, Germany) was used to automatically compensate for whole-cell capacitance and series resistance and perform voltage clamp protocols. Whole-cell currents were low-pass–filtered at 5 kHz and digitized at 50 kHz (45).

The holding potentials were −80 mV. The $Na^+$ currents ($I$) were elicited by test pulses ranging from −80 to +80 mV for 50 ms with increments of 10 mV. The amplitudes of transient sodium currents ($I_c$ and $I$) were recorded before and after the applications of different concentrations of AGAP and W38G. For determining the inhibition of peak current induced by AGAP and W38G, normalized current = $I/I_c$ was used. For determining the voltage dependence of activation, the sodium conductance was calculated using $G = I/(V_m - V_r)$, where $V_r$ is reversal potential. The $G$ value for each test potential was normalized to $G_{max}$ and plotted against the test potential to produce a voltage dependence of activation curves, which were fitted using Boltzmann functions, $G/G_{max} = 1/(1 + \exp((V_m - V_{½})/k))$, where $V_{½}$ is the voltage where half-maximal activation occurs, and $k$ is a slope factor. Inactivation curves were fitted with the Boltzmann equation, $I/I_{max} = 1/(1 + \exp((V_m - V_{½})/k))$, where $I/I_{max}$ is normalized current, $V_{½}$ is the potential for half-maximal inactivation, and $k$ is the slope factor. The time course of recovery of the sodium currents from inactivation was fitted with a tertiary exponential function, $I/I_{max} = A(1 - \exp(-\Delta t/\tau))$, where $I_{max}$ is the maximal current amplitude, $I$ is the current after a recovery period of $\Delta t$, $\tau$ is the time constant for recovery from inactivation, and $A$ is the amplitude coefficient.

### *Skeletal and cardiac toxicity of AGAP and W38G in vivo*

*Heart rate*—The mice were randomly divided into five groups of 10 individuals each: 1) normal saline control group; 2) AGAP, 2.5 mg/kg; 3) AGAP, 5.0 mg/kg; 4) W38G, 2.5 mg/kg; 5) W38G, 5.0 mg/kg. The heart rate was detected using an RM6240 multichannel physiological recorder. The mice were intravenously injected through the caudal vein within 10 s under anesthetic using pentobarbital sodium. The heart rate was counted from the start to 60 min of each group.

*Blood assays*—The mice were randomly divided into five groups of 10 individuals each: 1) normal saline control group; 2) AGAP, 2.5 mg/kg; 3) AGAP, 5.0 mg/kg; 4) W38G, 2.5 mg/kg; 5) W38G, 5.0 mg/kg. One hour after pretreatment, blood samples were collected from mice inner canthus in tubes and centrifuged at 6000 × *g* for 10 min, after which the serum fraction was transferred to another clean tube. Cardiac and skeletal muscle injury was assessed by determining the activity levels of serum CK and LDH using a CK detection kit (Beijing Solarbio Science and Technology) and LDH detection kit (Beijing Solarbio Science and Technology). Results are expressed in international units/liter.

*Forced swimming test*—The forced swimming exercise test was used as described previously with some modifications (46). Mice were pretreated with normal saline, AGAP (2.5 or 5.0 mg/kg), and W38G (2.5 or 5.0 mg/kg) once a day at the same time by intravenous injection within 10 s through the caudal vein for 7 consecutive days. 20 min after the last administration, an exhaustive swimming test was given. The surviving mice were placed individually in a columnar swimming pool (length 65 cm and radius 20 cm) with 40-cm water depth maintained at 28 ± 1 °C. A weight equivalent to 5% of body weight was attached to the root of the mouse tail, and the endurance for each mouse was measured as swimming times recorded from the beginning to exhaustion, which was determined by observing loss of coordinated movements and failure to return to the surface.

*Rotarod test*—The rotarod test was used as described previously with some modifications (47). One day before the test, the animals were trained twice. On the day of the test, only the mice that were able to stay balanced on the rotating rod between 80

and 120 s were selected for testing. The performance time was measured before and at 20 min after treatment. Mice were pretreated with saline, AGAP (2.5 or 5.0 mg/kg), and W38G (2.5 or 5.0 mg/kg) once a day at the same time by intravenous injection within 10 s through the caudal vein for 7 consecutive days. 20 min after the last administration, a rotarod test followed with a rod-rotating speed of 16 rpm. The integrity of motor coordination was assessed on the basis of endurance time of the animals on the rotating rod.

### *Analgesic effects of AGAP and W38G in vivo*

*Thermal pain test*—Female mice of 18–22 g were put on the hot plate, which was at a temperature of 55 ± 0.5 °C to induce pain. In response, the mice would lick or kick their feet, so that the time from putting the mice onto the hot plate to the licking or kicking action could be counted to reflect the intensity of pain. To perform the bioassay, samples were injected intravenously through the caudal vein in advance. Then the time was measured from putting it on the hot plate to its licking or kicking action at the 15, 30, 45, and 60 min. If this time was >60 s, the mice were taken away from the hot plate at once to prevent damage, and the time was counted as 60 s. The pain killer morphine was used as a positive control.

*Formalin-induced paw licking*—Pain was induced into mice by intraplantar injection of formalin, and pain attenuation was compared in mice injected intravenously through the caudal vein with either morphine, AGAP, W38G dissolved in 100 $\mu$l of saline. Control and normal saline mice received the same volume of saline. After a 15-min pretreatment, animals were injected with 10 $\mu$l of 2% (v/v) formalin at the plantar surface of the right hind paw, whereas normal saline mice were injected with 10 $\mu$l of saline. Mice were then placed individually into open polyvinyl cages. The time spent licking the injected paw was counted during phase I (0–5 min postinjection) and phase II (20–40 min postinjection). The painkiller morphine was used as a positive control.

### *Data analysis*

Statistical analysis of the data is provided as mean ± S.E. Group statistical significance was assessed using one-way ANOVA. Group statistical significance was assessed using log-rank test analysis in the survival experiment. $p < 0.05$ (*) and $p < 0.01$ (**) were considered statistically significant.

*Author contributions*—Y. X., X. M., X. H., and J. S. carried out electrophysiology studies. Y. X., J. S., Y. S., and Y. N. carried out toxicity experiments. Y. X., X. K., Y. S., and Z. L. carried out analgesic experiments. Y. M., Y. S., and Y. C. carried out peptide purification. Y. X., X. M., M. Z., and J. Z. conceived and designed the experiments. Y. X. and M. Z. wrote the manuscript, to which all authors contributed.

### References


1. Zlotkin, E., Miranda, F., and Rochat, H. (1978) Venoms of *Buthinae*: chemistry and pharmacology of *Buthinae* scorpion venoms. In *Arthropod Venoms* (Bettini, S., ed) pp. 317–369, Springer, New York
2. Possani, L. D. (1984) Structure of scorpion toxins. In *Handbook of Natural Toxins* (Tu, A. T., ed) pp. 513–550, CRC Press, New York
3. Zhou, X. H. (1984) The biochemical research on scorpion venoms and their application in therapy. *Progr. Biochem. Biophys.* **56,** 20–29
4. He, X., Peng, F., Zhang, J., Li, W., Zeng, X., and Liu, H. (2003) Inhibitory effects of recombinant neurotoxin BmK IM on seizures induced by pentylenetetrazol in rats. *Chin. Med. J.* **116,** 1898–1903
5. Liu, Y. F., Ma, R. L., Wang, S. L., Duan, Z. Y., Zhang, J. H., Wu, L. J., and Wu, C. F. (2003) Expression of an antitumor-analgesic peptide from the venom of Chinese scorpion Buthus martensii karsch in *Escherichia coli*. *Protein Expr. Purif.* **27,** 253–258
6. Chai, Z. F., Zhu, M. M., Bai, Z. T., Liu, T., Tan, M., Pang, X. Y., and Ji, Y. H. (2006) Chinese-scorpion (*Buthus martensi* Karsch) toxin BmK αIV, a novel modulator of sodium channels: from genomic organization to functional analysis. *Biochem. J.* **399,** 445–453
7. Zhao, R., Zhang, X. Y., Yang, J., Weng, C. C., Jiang, L. L., Zhang, J. W., Shu, X. Q., and Ji, Y. H. (2008) Anticonvulsant effect of BmK IT2, a sodium channel-specific neurotoxin, in rat models of epilepsy. *Br. J. Pharmacol.* **154,** 1116–1124
8. Cao, P., Yu, J., Lu, W., Cai, X., Wang, Z., Gu, Z., Zhang, J., Ye, T., and Wang, M. (2010) Expression and purification of an antitumor-analgesic peptide from the venom of *Mesobuthus martensii* Karsch by small ubiquitin-related modifier fusion in *Escherichia coli*. *Biotechnol. Prog.* **26,** 1240–1244
9. Du, J., Fu, Y., Wang, J., and Liang, A. (2013) Adenovirus-mediated expression of BmK CT suppresses growth and invasion of rat C6 glioma cells. *Biotechnol. Lett.* **35,** 861–870
10. Zhang, X. G., Wang, X., Zhou, T. T., Wu, X. F., Peng, Y., Zhang, W. Q., Li, S., and Zhao, J. (2016) Scorpion venom heat-resistant peptide protects transgenic *Caenorhabditis elegans* from β-amyloid toxicity. *Front. Pharmacol.* **7,** 227
11. Zhu, H., Wang, Z., Jin, J., Pei, X., Zhao, Y., Wu, H., Lin, W., Tao, J., and Ji, Y. (2016) Parkinson's disease-like forelimb akinesia induced by BmK I, a sodium channel modulator. *Behav. Brain Res.* **308,** 166–176
12. Cao, Z. Y., Mi, Z. M., Cheng, G. F., Shen, W. Q., Xiao, X., Liu, X. M., Liang, X. T., and Yu, D. Q. (2004) Purification and characterization of a new peptide with analgesic effect from the scorpion *Buthus martensi* Karch. *J. Pept. Res.* **64,** 33–41
13. Meng, X., Xu, Y., Wang, F., Zhao, M., Hou, X., Ma, Y., Jin, Y., Liu, Y., Song, Y., and Zhang, J. (2017) The roles of conserved aromatic residues (Tyr$^5$ and Tyr$^{42}$) in interaction of scorpion toxin BmK AGP-SYPU1 with human Nav1.7. *Int. J. Biol. Macromol.* **99,** 105–111
14. Chen, J., Feng, X. H., Shi, J., Tan, Z. Y., Bai, Z. T., Liu, T., and Ji, Y. H. (2006) The anti-nociceptive effect of BmK AS, a scorpion active polypeptide, and the possible mechanism on specifically modulating voltage-gated $Na^+$ currents in primary afferent neurons. *Peptides* **27,** 2182–2192
15. Lin, S., Wang, X., Hu, X., Zhao, Y., Zhao, M., Zhang, J., and Cui, Y. (2017) Recombinant expression, functional characterization of two scorpion venom toxins with three disulfide bridges from the Chinese scorpion *Buthus martensii* Karsch. *Protein Pept. Lett.* **24,** 235–240
16. Deng, Y. P., Xu, G. Z., Wang, W., Shen, X. H., Chen, Q. T., Gao, H. Z., Pan, Y. Z., Zhu, T. Y., Zhu, D. M., Zhou, X. M., Liu, Y. L., and Cai, Z. J. (2002) Clinical evaluation of analgesic effect and safety of scorpion venom injection. *Chin. Pharm. J.* **37,** 459–462
17. Zaharieva, I. T., Thor, M. G., Oates, E. C., van Karnebeek, C., Hendson, G., Blom, E., Witting, N., Rasmussen, M., Gabbett, M. T., Ravenscroft, G., Sframeli, M., Suetterlin, K., Sarkozy, A., D'Argenzio, L., Hartley, L., *et al.* (2016) Loss-of-function mutations in SCN4A cause severe foetal hypokinesia or "classical" congenital myopathy. *Brain* **139,** 674–691
18. Sheets, P. L., Heers, C., Stoehr, T., and Cummins, T. R. (2008) Differential block of sensory neuronal voltage-gated sodium channels by lacosamide [(2*R*)-2-(acetylamino)-*N*-benzyl-3–3-methoxypropana mide], lidocaine, and carbamazepine. *J. Pharmacol. Exp. Ther.* **326,** 89–99
19. Anger, T., Madge, D. J., Mulla, M., and Riddall, D. (2001) Medicinal chemistry of neuronal voltage-gated sodium channel blockers. *J. Med. Chem.* **44,** 115–137
20. Royer, A., van Veen, T. A., Le Bouter, S., Marionneau, C., Griol-Charhbili, V., Léoni, A. L., Steenman, M., van Rijen, H. V., Demolombe, S., Goddard, C. A., Richer, C., Escoubet, B., Jarry-Guichard, T., Colledge, W. H., Gros, D., *et al.* (2005) Mouse model of SCN5A-linked hereditary Lenegre's disease: age-related conduction slowing and myocardial fibrosis. *Circulation* **111,** 1738–1746

21. Márquez, M. F., Bonny, A., Hernández-Castillo, E., De Sisti, A., Gómez-Flores, J., Nava, S., Hidden-Lucet, F., Iturralde, P., Cárdenas, M., and Tonet, J. (2012) Long-term efficacy of low doses of quinidine on malignant arrhythmias in Brugada syndrome with an implantable cardioverter-defibrillator: a case series and literature review. *Heart Rhythm* **9,** 1995–2000
22. King, J. H., Huang, C. L., and Fraser, J. A. (2013) Determinants of myocardial conduction velocity: implications for arrhythmogenesis. *Front. Physiol.* **4,** 154
23. Mao, Q., Ruan, J., Cai, X., Lu, W., Ye, J., Yang, J., Yang, Y., Sun, X., Cao, J., and Cao, P. (2013) Antinociceptive effects of analgesic-antitumor peptide (AGAP), a neurotoxin from the scorpion *Buthus martensii* Karsch, on formalin-induced inflammatory pain through a mitogen-activated protein kinases-dependent mechanism in mice. *PLoS One* **8,** e78239
24. Cui, Y., Guo, G. L., Ma, L., Hu, N., Song, Y. B., Liu, Y. F., Wu, C. F., and Zhang, J. H. (2010) Structure and function relationship of toxin from Chinese scorpion *Buthus martensii* Karsch (BmKAGAP): gaining insight into related sites of analgesic activity. *Peptides* **31,** 995–1000
25. Quintero-Hernández, V., Ramírez-Carreto, S., Romero-Gutiérrez, M. T., Valdez-Velázquez, L. L., Becerril, B., Possani, L. D., and Ortiz, E. (2015) Transcriptome analysis of scorpion species belonging to the *Vaejovis* genus. *PLoS One* **10,** e0117188
26. Santibáñez-López, C. E., and Possani, L. D. (2015) Overview of the Knottin scorpion toxin-like peptides in scorpion venoms: insights on their classification and evolution. *Toxicon* **107,** 317–326
27. Galen, R. S. (1975) The enzyme diagnosis of myocardial infarction. *Hum. Pathol.* **6,** 141–155
28. Roark, S. F., Wagner, G. S., Izlar, H. L., Jr., and Roe, C. R. (1976) Diagnosis of acute myocardial infarction in a community hospital. *Circulation* **53,** 965–969
29. Henderson, A. R., and Moss, D. W. (1986) Enzymes. In *Tietz Fundamentals of Clinical Chemistry*, 5th Ed. (Burtis, C. A., and Ashwood, E. R., eds) pp. 356–366, Elsevier, Philadelphia
30. Alpert, J. S., Thygesen, K., Antman, E., and Bassand, P. J. (2000) Myocardial infarction redefined a consensus document of the Joint European Society of Cardiology Committee for the redefinition of myocardial infarction. *J. Am. Coll. Cardiol.* **36,** 959–969
31. Lewandrowski, K., Chen, A., and Januzzi, J. (2002) Cardiac markers for myocardial infarction: a brief review. *Am. J. Clin. Pathol.* **118,** S93–S99
32. Nathwani, R. A., Pais, S., Reynolds, T. B., and Kaplowitz, N. (2005) Serum alanine aminotransferase in skeletal muscle diseases. *Hepatology* **41,** 380–382
33. Black, J. A., Dib-Hajj, S., McNabola, K., Jeste, S., Rizzo, M. A., Kocsis, J. D., and Waxman, S. G. (1996) Spinal sensory neurons express multiple sodium channel $\alpha$-subunit mRNAs. *Brain Res. Mol. Brain Res.* **43,** 117–131
34. Sangameswaran, L., Fish, L. M., Koch, B. D., Rabert, D. K., Delgado, S. G., Ilnicka, M., Jakeman, L. B., Novakovic, S., Wong, K., Sze, P., Tzoumaka, E., Stewart, G. R., Herman, R. C., Chan, H., Eglen, R. M., and Hunter, J. C. (1997) A novel tetrodotoxin-sensitive, voltage-gated sodium channel expressed in rat and human dorsal root ganglia. *J. Biol. Chem.* **272,** 14805–14809
35. Toledo-Aral, J. J., Moss, B. L., He, Z. J., Koszowski, A. G., Whisenand, T., Levinson, S. R., Wolf, J. J., Silos-Santiago, I., Halegoua, S., and Mandel, G. (1997) Identification of PN1, a predominant voltage-dependent sodium channel expressed principally in peripheral neurons. *Proc. Natl. Acad. Sci. U.S.A.* **94,** 1527–1532
36. Yang, S., Xiao, Y., Kang, D., Liu, J., Li, Y., Undheim, E. A., Klint, J. K., Rong, M., Lai, R., and King, G. F. (2013) Discovery of a selective NaV1.7 inhibitor from centipede venom with analgesic efficacy exceeding morphine in rodent pain models. *Proc. Natl. Acad. Sci. U.S.A.* **110,** 17534–17539
37. Thomas-Tran, R., and Du Bois, J. (2016) Mutant cycle analysis with modified saxitoxins reveals specific interactions critical to attaining high-affinity inhibition of hNaV1.7. *Proc. Natl. Acad. Sci. U.S.A.* **113,** 5856–5861
38. Vetter, I., Deuis, J. R., Mueller, A., Israel, M. R., Starobova, H., Zhang, A., Rash, L. D., and Mobli, M. (2017) NaV1.7 as a pain target: from gene to pharmacology. *Pharmacol. Ther.* **172,** 73–100
39. Dib-Hajj, S. D., Yang, Y., Black, J. A., and Waxman, S. G. (2013) The Na(v)1.7 sodium channel: from molecule to man. *Nat. Rev. Neurosci.* **14,** 49–62
40. Cox, J. J., Reimann, F., Nicholas, A. K., Thornton, G., Roberts, E., Springell, K., Karbani, G., Jafri, H., Mannan, J., Raashid, Y., Al-Gazali, L., Hamamy, H., Valente, E. M., Gorman, S., Williams, R., McHale, D. P., Wood, J. N., Gribble, F. M., and Woods, C. G. (2006) An SCN9A channelopathy causes congenital inability to experience pain. *Nature* **444,** 894–898
41. Akopian, A. N., Sivilotti, L., and Wood, J. N. (1996) A tetrodotoxin resistant voltage-gated sodium channel expressed by sensory neurons. *Nature* **379,** 257–262
42. Sangameswaran, L., Delgado, S. G., Fish, L. M., Koch, B. D., Jakeman, L. B., Stewart, G. R., Sze, P., Hunter, J. C., Eglen, R. M., and Herman, R. C. (1996) Structure and function of a novel voltage-gated, tetrodotoxin-resistant sodium channel specific to sensory neurons. *J. Biol. Chem.* **271,** 5953–5956
43. Joshi, S. K., Mikusa, J. P., Hernandez, G., Baker, S., Shieh, C. C., Neelands, T., Zhang, X. F., Niforatos, W., Kage, K., Han, P., Krafte, D., Faltynek, C., Sullivan, J. P., Jarvis, M. F., and Honore, P. (2006) Involvement of the TTX-resistant sodium channel Nav1.8 in inflammatory and neuropathic, but not post-operative, pain states. *Pain* **123,** 75–82
44. Cestèle, S., Qu, Y., Rogers, J. C., Rochat, H., Scheuer, T., and Catterall, W. A. (1998) Voltage sensor-trapping: enhanced activation of sodium channels by $\beta$-scorpion toxin bound to the S3-S4 loop in domain II. *Neuron* **21,** 919–931
45. Kahlig, K. M., Lepist, I., Leung, K., Rajamani, S., and George, A. L. (2010) Ranolazine selectively blocks persistent current evoked by epilepsy-associated Nav1.1 mutations. *Br. J. Pharmacol.* **161,** 1414–1426
46. Porsolt, R. D., Le Pichon, M., and Jalfre, M. (1977) Depression: a new animal model sensitive to antidepressant treatments. *Nature* **266,** 730–732
47. Galeotti, N., Ghelardini, C., Caldari, B., and Bartolini, A. (1999) Effect of potassium channel modulators in mouse forced swimming test. *Br. J. Pharmacol.* **126,** 1653–1659